

Phase Differences Determination between the Fundamental and Higher Harmonic Components at Non-coherent Sampling

David Slepíčka

*Dept. of Measurement, Faculty of Electrical Engineering, Czech Technical University in Prague,
Technická 2, CZ-16627 Prague 6, Czech Republic
Phone: ++ 420 2 2435 2058, Fax: ++ 420 2 3333 9929, E-mail: slepiced@fel.cvut.cz*

Abstract – The main product of the DFT algorithms is the amplitude frequency spectrum while the phase frequency spectrum calculation is mainly unwanted. However, this part becomes relevant in the cases, in which the spectral lines have to be considered as vectors. Since the data record, from which the frequency spectrum is calculated, is usually acquired by non-coherent sampling, a problem of the correct phase determination appears. Time windows minimise the leakage in the amplitude frequency spectrum; their effect on the phase frequency spectrum is unclear. Moreover, the phase of each frequency depends on its initial phase and it varies in every data record, which is often undesired. One possibility of how to exactly express the phases of higher harmonic components is described in this paper.

I. Rectangular window

The amplitude frequency spectrum as well as the phase frequency spectrum strongly depend on the time window used. Sampling without application of any window can be described as a multiplication of the sampled signal by rectangular window or by the sequence of unitary discrete pulses. The frequency spectrum of the window is given by

$$X_{rec}(e^{j\theta\frac{2\pi}{N}}) = \sum_{n=0}^{N-1} e^{-jn\theta\frac{2\pi}{N}} = \frac{1 - e^{-j\theta 2\pi}}{1 - e^{-j\theta\frac{2\pi}{N}}} = \frac{\sin \theta\pi}{\sin \theta\frac{\pi}{N}} e^{-j\theta\pi\frac{N-1}{N}}, \quad (1)$$

where N is the number of samples and θ is the normalized frequency $\theta = fT$ (f is the frequency and T the window length). The main lobe of this window is narrow enabling a high distinction of neighbouring frequency lines but the amplitudes of side lobes fall slowly at the rate described by $\sin(\theta\pi/N)$ and influence amplitude frequency spectrum (see Fig. 1a).

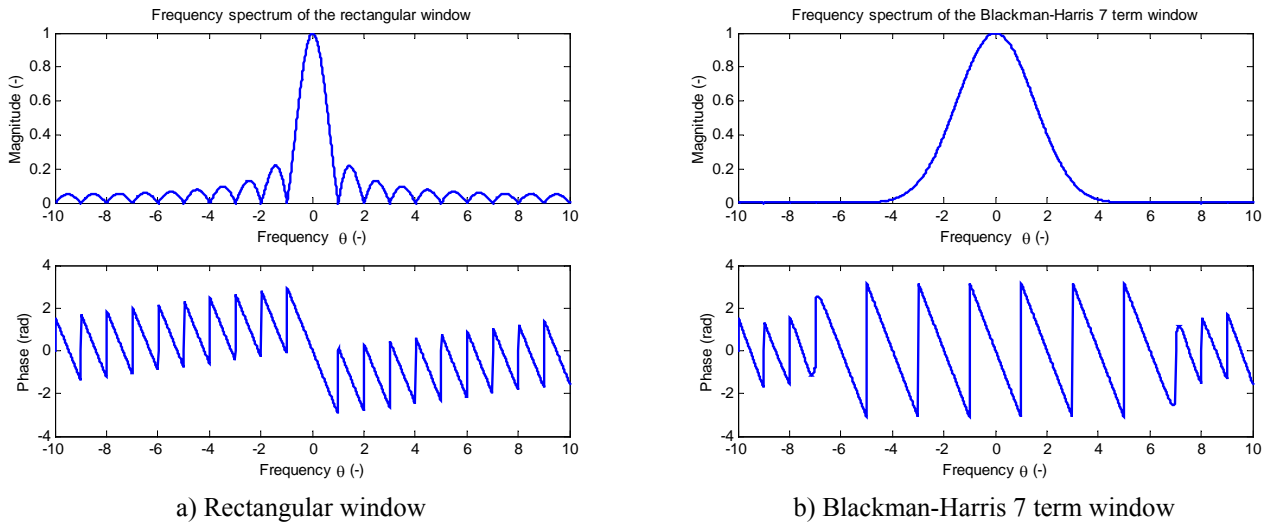


Fig. 1 Frequency spectra of some time windows

The integer parts of normalized frequency θ correspond to the frequency bins which are visible in discrete spectral analysis. An example of discrete frequency spectrum modified by the rectangular window is demonstrated by the signal

$$x(n) = \frac{1}{2} e^{20.4j\frac{2\pi}{N}n}, \quad (2)$$

where n is the sample order. Actually, it is a common sine (cosine) signal, from which the negative frequency term has been eliminated:

$$\cos\left(20.4 \frac{2\pi}{N} n\right) = \frac{1}{2} e^{20.4j \frac{2\pi}{N} n} + \frac{1}{2} e^{-20.4j \frac{2\pi}{N} n} \quad (3)$$

The influence of this negative frequency term is significant especially in the phase frequency spectrum. It can be neglected in the amplitude frequency.

The operation of windowing is the multiplication of the signal $x(n)$ by the window $w(n)$. The signal $x(n)$ is the complex exponential function in this case. Generally, the multiplication by the complex exponential function $e^{j \frac{2\pi}{N} n k_0}$ in the time domain causes the frequency shift k_0 in the frequency domain. The coefficient k_0 is the number of samples per period which is the constant 20.4. The result of the rectangular window application on this signal in the discrete domain is determined by

$$X(k) = \sum_{n=0}^N \frac{1}{2} e^{20.4j \frac{2\pi}{N} n} \cdot e^{-j \frac{2\pi}{N} nk} = \frac{1 - e^{-j2\pi(k-20.4)}}{1 - e^{-j \frac{2\pi}{N}(k-20.4)}} \quad (4)$$

The operation described above can be performed as the sampling in the frequency domain as well (see Fig. 2a). In the discrete amplitude frequency spectrum leakage is visible; in the phase frequency spectrum a step of π appear between two frequency bins adjacent to the nominal frequency 20.4. If the sampling is coherent, all discrete phases would be zero except the phase of the nominal frequency which would correspond to the phase at the time the sampling starts.

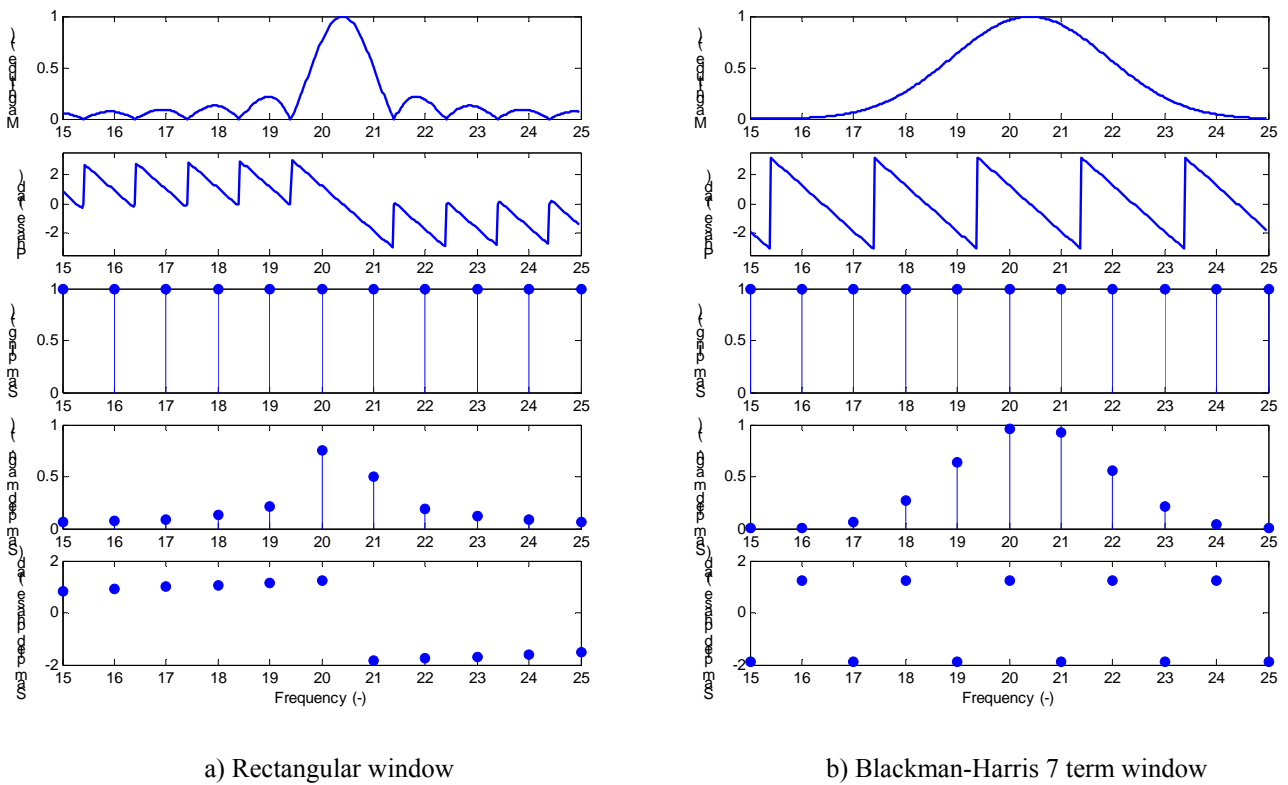


Fig. 2 Influence of some time windows on the frequency spectrum

Side lobes suppression of the used window has a significant influence not only on the correct determination of the amplitude frequency spectrum of the sampled signal but also on the exact interpretation of the phase frequency spectrum. Signals with smaller amplitude will not be visible. Consequently, it is difficult to determine the phases of such signals as well.

There is a demonstration of the time windows influence on a non-coherently sampled signal with the fundamental and two higher harmonics and zero phases in the Fig. 3:

$$x(n) = \cos\left(20.4 \frac{2\pi}{N} n\right) + \frac{1}{2} \cos\left(2 \cdot 20.4 \frac{2\pi}{N} n\right) + \frac{1}{3} \cos\left(3 \cdot 20.4 \frac{2\pi}{N} n\right). \quad (5)$$

This signal was multiplied by the rectangular window and its frequency spectrum calculated (Fig. 3a). The side lobes' amplitudes of this window cause a distortion of neighbouring frequency spectral lines. The amplitude frequency spectrum lines, which belong to higher harmonic components contained in the signal, are distorted as are the phase frequency spectrum lines. For the correct determination of each frequency line, the side lobes' influence has to be taken into account, a process which is rather complicated.

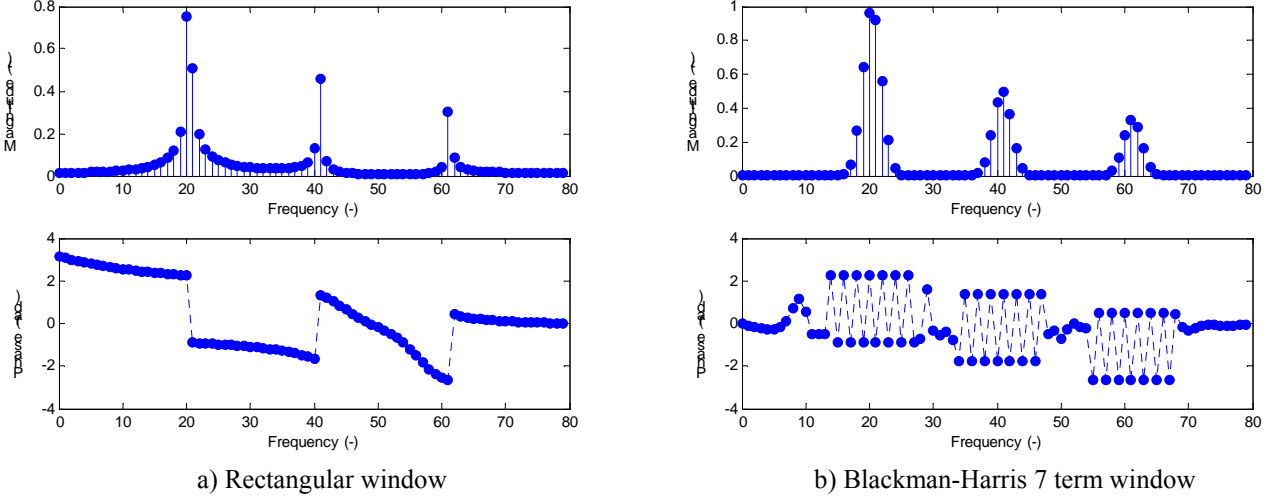


Fig. 3 Frequency spectra of the windowed signal with higher harmonics

II. Cosine windows

To suppress the leakage effect as much as possible, the sampled signal is multiplied by cosine time window $w_{\cos}(t)$ before the frequency spectrum computation

$$w_{\cos}(t) = \sum_{l=0}^{L-1} (-1)^l a_l \cos \frac{2\pi}{T} tl, \quad (6)$$

where L is the window order and T its length. The window order determines the main lobe width and the suppression of side lobes. The frequency spectrum of this window can be computed as [1]

$$X_{\cos}(f) = \frac{1}{T} \int_0^T \sum_{l=0}^{L-1} (-1)^l a_l \cos \frac{2\pi}{T} tl \cdot e^{-j2\pi ft} dt = [\sin(2\pi\theta) + j(\cos(2\pi\theta) - 1)] \frac{1}{2\pi} \sum_{l=0}^{L-1} (-1)^l a_l \frac{\theta}{\theta^2 - l^2}, \quad (7)$$

where $\theta = fT$. For the ADC testing, the Blackman-Harris 7 term window (see [2] for coefficients values) is often used ($L = 7$; the peak of highest side lobe is -191.45 dB [2]). Fig. 1b shows the frequency spectrum of this window. The important part of the spectrum is only in the range within ± 6 frequency bins (window order minus one) around the basic frequency because the suppression gain of the window at other frequencies is too high. The phase frequency spectrum of this window can be computed as

$$\phi_{BH7}(\theta) = \arctan \left(\frac{\cos(2\pi\theta) - 1}{\sin(2\pi\theta)} \operatorname{sign} \left(\sum_{l=0}^{L-1} (-1)^l a_l \frac{\theta}{\theta^2 - l^2} \right) \right). \quad (8)$$

The sign function within the range $\pm 6\theta$ is a rectangular function ± 1 which changes its value at the frequencies where θ is an integer. This is the characteristics of the window coefficients a_l . Each a_l is mostly significant for $\theta \approx l$; at the frequency of $\theta = l$ it changes the sign in the fragment denominator. The function of the sum argument $X = \sum_{l=0}^{L-1} (-1)^l a_l \frac{\theta}{\theta^2 - l^2}$ for this window coefficients a_l is shown in Fig. 4. Thus, this sign function can be simplified by $\operatorname{sign}(\sin(\pi\theta))$. The phase spectrum (with regard to all phase quadrants – see Fig. 1b) is then

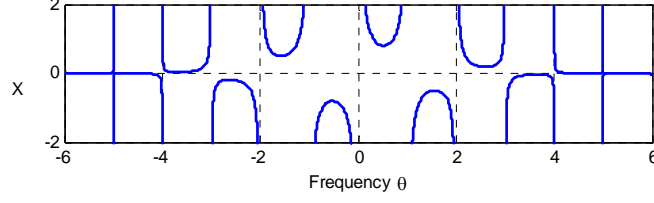


Fig. 4 Argument of the sign function

$$\phi_{BH7}(\theta) = \arctan\left(\frac{-\sin^2(\pi\theta)}{\sin(\pi\theta)\cos(\pi\theta)} \text{sign}(\sin(\pi\theta))\right) = -\pi\theta. \quad (9)$$

The influence of this window on the non-coherently sampled complex exponential function (2) is shown in Fig. 2b). One original line in the amplitude frequency spectrum is scattered in several adjacent lines but the long-range leakage is eliminated. The phase frequency spectrum alternates between two values shifted by π at the range $\pm 6\theta$ around a significant spectral line. It is the result of the convolution of the cosine window (6) and the signal (2).

Fig. 3b) shows the demonstration of the influence of the Blackman-Harris 7 term window on the non-coherently sampled signal with three harmonic components. The side lobe energy can be neglected; therefore, the amplitudes and phases of all significant harmonic components can be determined without loss of accuracy. To determine correctly two neighbouring frequency spectral lines, their distance has to be at least the number of frequency bins equal to the window order L .

III. Phase differences determination

In practice, the sampling is not usually synchronized with the fundamental frequency. Thus, the phase of each frequency depends on the initial phase at the time of the beginning of the sampling. The absolute phase determination of a specific frequency contributes no information. To obtain an information about the signal, the phase has to be determined relatively using a reference signal. This reference signal has to be coherent with the signals being referenced and should have equal or lower frequency for the unambiguous interpretation. The fundamental harmonic fulfils the characteristics described above. It was used as the reference signal in this research.

The phase difference $\Delta\phi_{lh}$ between the absolute phase of the h -th harmonic component and the fundamental harmonic component can be computed as

$$\Delta\phi_{lh} = \phi_h - h \cdot \phi_1. \quad (10)$$

The multiplication of the fundamental frequency phase by the harmonic component order corrects different lengths of period.

Consider a real discrete signal of a fundamental frequency and its h -th harmonic component of smaller amplitude

$$x(n) = \cos\left((a + \alpha)\frac{2\pi}{N}n + \varphi_1\right) + \cos\left(h(a + \alpha)\frac{2\pi}{N}n + \varphi_h\right). \quad (11)$$

where $(a + \alpha)$ is the number of samples of the fundamental frequency in one period, φ is the initial phase, a is integer and $|\alpha| \leq 0,5$. The amplitude frequency spectrum reaches its maximum at the frequency bin a . The phase spectrum (Blackman-Harris 7 term window) is

$$\phi_1 = \phi_{BH7}(-\alpha) + \varphi_1 = \alpha\pi + \varphi_1, \quad (12)$$

which results from the convolution and the frequency spectrum shift $\pm(a + \alpha)$ and its sampling at the frequency bin a (the influence of the negative term can be neglected). The phase at the frequency bin ha is similarly

$$\phi_h = \phi_{BH7}(-h\alpha) + \varphi_h = h\alpha\pi + \varphi_h. \quad (13)$$

The difference (10) of two previous phases is then

$$\Delta\phi_{lh} = \phi_h - h\phi_1 = h\alpha\pi + \varphi_h - h(\alpha\pi + \varphi_1) = \varphi_h - h\varphi_1, \quad (14)$$

which corresponds to the actual phase difference. Note, it does not depend on α and thus the non-coherency.

IV. Algorithm of the phase differences computation

The phase differences determination mentioned above computes the phase of the harmonic component h at the frequency ha and does not consider the term α (the correct frequency should be $h(a + \alpha)$). The error is mostly not high for low values of

harmonic order h because of the phase linearity of the window within ± 6 frequency bins ($h\alpha < 6$) around the correct higher harmonic frequency – see Fig. 2b). This frequency will be out of the range for higher h , so the determined phase will no longer correspond to the correct phase.

The term α is usually unknown. Nevertheless, the nearest frequency bin of the harmonic component h can be estimated as the local maximum of the amplitude frequency characteristics. Even then the correct phase is unclear because the phase decreases with π between two adjacent frequency bins due to the used window. Thus, each second frequency bin has the same phase. The algorithm for the most common case of the dominant fundamental harmonic is shown in Fig. 5.

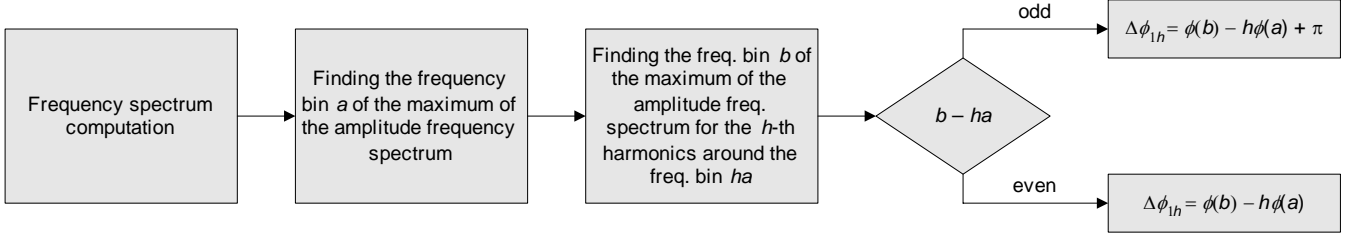


Fig. 5 Algorithm of the phase differences computation

An example of the algorithm implementation mentioned above is shown in Fig. 6. A non-coherently sampled rectangular signal without DC component was applied. Note, the phases in Fig. 6 are calculated for cosine functions, not sine functions.

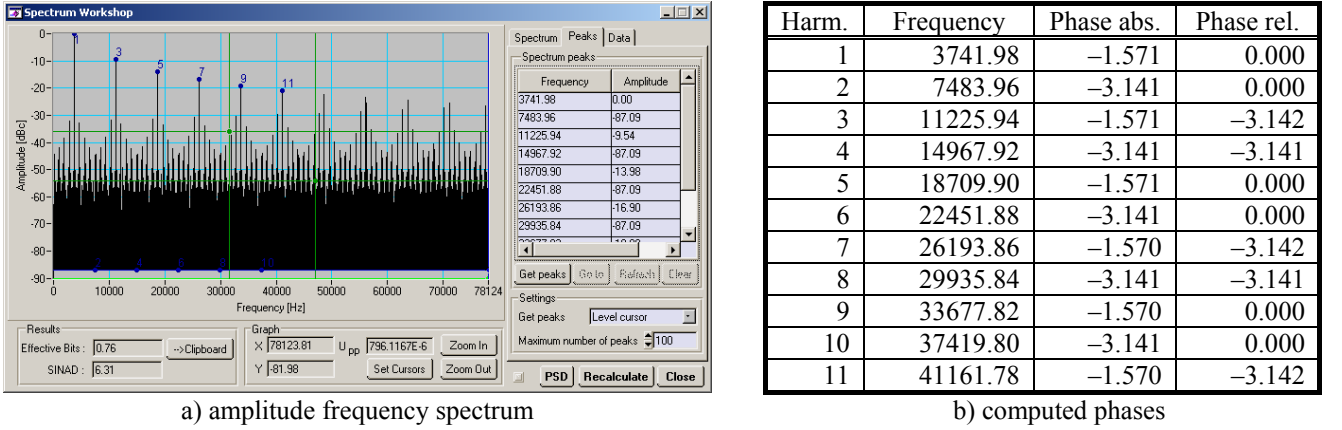


Fig. 6 Phases computation of a non-coherently sampled rectangular function

V. Uncertainty analysis

The phases are determined by the frequency spectrum $X(k)$ which can be computed from a sequence of samples $x(n)$ by the DFT algorithm. Cosine time window $w_{\cos}(t)$ is also applied:

$$X(k) = \frac{1}{N} \sum_{n=0}^{N-1} x(n) w_{\cos}(n) e^{-\frac{2\pi}{N}nk} \quad (15)$$

This can be gained as the composition [3] of the real $R(k)$ and imaginary $I(k)$ part $X(k) = R(k) + I(k)$

$$R(k) = \frac{1}{N} \sum_{n=0}^{N-1} x(n) w_{\cos}(n) \cos\left(\frac{2\pi}{N}nk\right), \quad I(k) = -\frac{1}{N} \sum_{n=0}^{N-1} x(n) w_{\cos}(n) \sin\left(\frac{2\pi}{N}nk\right). \quad (16), (17)$$

Uncertainties of both parts are given by

$$u_{R(k)}^2 = \left[\frac{\partial R(k)}{\partial x(n)} \right]^2 u_{x(n)}^2 = \frac{u_q^2}{2N^2} \left[N \cdot NNPG + \sum_{n=0}^{N-1} \cos\left(\frac{4\pi}{N}nk\right) w_{\cos}^2(n) \right], \quad (18)$$

$$u_{I(k)}^2 = \left[\frac{\partial I(k)}{\partial x(n)} \right]^2 u_{x(n)}^2 = \frac{u_q^2}{2N^2} \left[N \cdot NNPG - \sum_{n=0}^{N-1} \cos\left(\frac{4\pi}{N}nk\right) w_{\cos}^2(n) \right], \quad (19)$$

where u_q is the quantization uncertainty and $NNPG$ normalized noise power gain (noise power gain divided by that of the rectangular window) equal to

$$u_q = \frac{U_{FS}}{2^{ENOB} \sqrt{12}}, \quad NNPG = \frac{1}{N} \sum_{n=0}^{N-1} w_{\cos}^2(n). \quad (20), (21)$$

where $ENOB$ is the effective number of bits and U_{FS} is the full-scale range of the used ADC.

The module $M(k)$ and phase $\phi(k)$ are

$$M(k) = \sqrt{R^2(k) + I^2(k)}, \quad \phi(k) = \arctg\left(\frac{I(k)}{R(k)}\right). \quad (22), (23)$$

The phase uncertainty is given by

$$u_{\phi(k)}^2 = \left[\frac{\partial \phi(k)}{\partial R(k)} \right]^2 u_{R(k)}^2 + \left[\frac{\partial \phi(k)}{\partial I(k)} \right]^2 u_{I(k)}^2 + 2 \left[\frac{\partial \phi^2(k)}{\partial R(k) \partial I(k)} \right]^2 u_{[R(k), I(k)]}^2, \quad (24)$$

where

$$u_{[R(k), I(k)]}^2 = \sum_{n=0}^{N-1} \frac{\partial R(k)}{\partial x(n)} \frac{\partial I(k)}{\partial x(n)} u_x^2(n) = -\frac{u_q^2}{N} \sum_{n=0}^{N-1} \sin\left(\frac{4\pi}{N} nk\right) w_{\cos}^2(n) = 0. \quad (25)$$

Therefore

$$u_{\phi(k)}^2 = \frac{u_q^2}{2N^2 M^4} \left[N \cdot M^2 \cdot NNPG + \sum_{n=0}^{N-1} \cos\left(\frac{4\pi}{N} nk\right) w_{\cos}^2(n) (I^2(k) - R^2(k)) \right]. \quad (26)$$

It can be derived that the second term (sum) is zero for values of k within the interval $\langle L; N/2 - L \rangle$, where L is the window order (for k in $0 \dots N/2$ and even number of samples N). The phase uncertainty is then

$$u_{\phi(k)}^2 = \frac{u_q^2}{2N \cdot M^2} NNPG. \quad (27)$$

So, it does not depend on k . Applying the (27), the uncertainty of the phase difference is given by

$$u_{\Delta\phi_h}^2 = \left(\frac{\partial \Delta\phi_h}{\partial \phi_h} \right)^2 u_{\phi_h}^2 + \left(\frac{\partial \Delta\phi_h}{\partial \phi_l} \right)^2 u_{\phi_l}^2 = u_{\phi_h}^2 + h^2 u_{\phi_l}^2 = (h^2 + 1) \frac{u_q^2}{2N \cdot M^2} NNPG; \quad (28)$$

the phases ϕ_h and ϕ_l are supposed to be independent.

VI. Conclusion

The algorithm described in this paper enables phase differences determination by non-coherent sampling using the Blackman-Harris 7 term window. It was developed for frequency spectrum correction in ADC testing, which has to be performed with regard to both frequency amplitude and phase. It could be also used e.g. for system diagnostics because phase change is usually more distinct than amplitude change.

References

- [1] H. H. Albrecht "A Family of Cosine-Sum Windows for High-Resolution Measurements". IEEE Proc. ICASSP2001, May 7–11, 2001 Salt Lake City, UT, USA.
- [2] O. M. Solomon, Jr. "The Use of DFT Windows in Signal-to-Noise Ratio and Harmonic Distortion Computations". IEEE Transactions on Instrumentation and Measurement, April 1994, vol. 43, pp 194–199.
- [3] G. Betta, C. Liguori, A. Pietrosanto "Uncertainty Analysis in Fast Fourier Transform Algorithms". IMEKO TC-4, September 17–18, 1998 Naples, Italy, pp 747–752.
- [4] IEEE Std. 1057–1994: *IEEE standard for digitising waveform recorders*. The Institute of electrical and Electronics Engineers, Inc., New York, 1994.
- [5] IEEE Std. 1241–2000: *IEEE Standard for Terminology and Test Methods for Analog-to-Digital Converters*. The Institute of Electrical and Electronics Engineers, Inc., New York, 2000.